

Hemodynamics in a time-dependent, bell-shaped stenosed artery

Jeevan Kafle¹, Biddha Pokhrel¹, Pushpa Nidhi Gautam^{1,2,*}

¹Central Department of Mathematics,
Institute of Science and Technology, Tribhuvan University, Nepal
jeevan.kafle@cdmath.tu.edu.np
pokhrelbidhya2001@gmail.com

²Department of Mathematics,
Patan Multiple Campus, Tribhuvan University, Nepal
pushpa.gautam@pmc.tu.edu.np

Received: 27 June 2025, Published: 1 May 2026

Abstract: The dynamics of blood flow are dramatically changed by arterial stenosis, a leading cause of cardiovascular diseases. The hemodynamics through a bell-shaped stenosis are examined in this work, which increases with time. A new model is developed after incorporating the temporal term in the geometry of the bell-shaped stenosis. The equation is then solved to get analytical solutions of the flow parameters for axisymmetric, incompressible, and fully developed flow, taking blood as a non-Newtonian fluid. Important variables, including viscosity, time, and stenosis geometry, are changed to see how they affect the volumetric flow rate, velocity, pressure drop, pressure drop ratio, shear stress, and shear stress ratio. The findings demonstrate a large drop in velocity and volumetric flow rate at the bell-shaped stenotic region with increasing time and viscosity. In the region of bell-shaped stenosis, pressure drop and wall shear stress and their ratios increase rapidly with increasing stenosis. These results demonstrate how important the bell-shaped progressive stenosis is to prevent blood flow and raise the risk of cardiovascular disease. It can be used for the clinical approach and for the researchers in this field.

Keywords: bell-shaped stenosis, shear-thinning behavior, power-law, non-Newtonian fluid, Navier-Stokes equations

I. INTRODUCTION

Blood is a complicated biological fluid that supplies oxygen and nutrients to tissues and cells, which is essential for preserving human health [1,2]. Blood contains suspended blood cells in plasma. It can be treated as a non-Newtonian fluid, whose viscosity changes with the shear rate and which is heterogeneous, making the flow complicated [3]. Blood reaches every cell of the body with the help of arteries, which are a closed network of vessels, which vary in size and usually tapering in nature [4]. The largest of these arteries is the aorta which is about 2.5 cm in diameter, and the capillaries are very small in size, which are less than 5 μm in diameter [5]. Arteries have different geometrical structures, such as branching, curvature, and tapering in size, and that makes the flow complicated [6]. It is necessary to know the arterial network and its structure to understand cardiovascular diseases, especially those associated with structural anomalies such as stenosis or narrowing of the arterial lumen and inner artery walls [7,8].

Copyright: © 2026 Jeevan Kafle, Biddha Pokhrel, Pushpa Nidhi Gautam. This article is distributed under the terms of the Creative Commons Attribution License (CC BY 4.0), which permits unrestricted use, distribution, and reproduction in any medium, provided the original author and source are credited. *Corresponding author

Citation: Jeevan Kafle, Biddha Pokhrel, Pushpa Nidhi Gautam, Hemodynamics in a time-dependent, bell-shaped stenosed artery, Biomath 15 (2026), 2605014, <https://doi.org/10.55630/j.biomath.2026.05.014> 1/12

Further on, all flow parameters of blood flow through a curved artery having symmetric shaped stenosis were already calculated by Gautam and Kafle in [9].

Stenosis modifies the normal circulation of blood and affects the flow parameters such as velocity profile, volumetric flow rate, pressure drop, pressure drop ratio, wall shear stress, and its ratio [10–12]. Due to the sharp wall, the bell-shaped stenosis has a significant impact on the blood flow dynamics and the temporal term, which measures the rate of increasing thickness, making this model more effective.

According to Young [13], the impact of stenosis becomes considerable when it surpasses the critical value. Low shear stress is strongly associated with plaque buildup, which suggests critical shear level may play a key role in its development [14]. Lee and Fung [15] investigated the flow dynamics within a constricted tube, focusing on steady flow conditions characterized by a low Reynolds number.

Kafle et al. [16] discuss and derive analytical solutions for flow variables including velocity, volumetric flow rate, and pressure drop in the stenosed portion of an artery. Muravyov et al. [17] have stated that hydrogen sulfide and sodium nitroprusside help to make erythrocytes more deformable when gasotransmitter donors are involved. The impacts of vorticity and velocity characteristics at the apex of the bifurcation in the stenotic region have been explored by Antonova et al. [18].

After studying the effect of time-varying curvature on the velocity profile, Schilt et al. [19] came to the conclusion that the curvature causes the velocity profile to change in form and be biased against the outer wall. Gautam et al. [20] investigated the effect of curvature on flow parameters using analytical solutions in a two-layered model.

Amit et al. [21] modeled the blood flow in an arterial segment considering the combined effects of time-varying stenosis and slip boundary conditions. Particularly in tiny arteries or at low shear rates, blood exhibits non-Newtonian behavior [22, 23]. Under these circumstances, its viscosity varies according to the shear rate [2, 17]. A popular model for explaining this behavior is the power-law model, which describes blood as a fluid that thins with shear [2, 17]. For this model, the velocity distribution is determined by a flow behavior index n , where shear-thinning behavior is indicated by $n < 1$ [24, 25].

Blood flow through a bell-shaped narrowing catheterized artery is analyzed by Srivastav and Agnihotri [26], considering blood as a Newtonian fluid, and they

have shown that the flow resistance and shear stress increase with increasing catheter and stenosis size, and shear stress at the throat behaves like impedance. In spite of these developments, most previous studies have employed static stenosis models or simplified sinusoidal temporal variations.

Gautam et al. [27] have calculated the flow parameters for a stenosis increasing with time and symmetric in shape. Ponalagusamy and Manchi [28] have examined the flow behavior of six different types of stenosis, including bell-shaped taking blood as a K-L Newtonian fluid. Very little is known about the combined consequences of time-dependent and bell-shaped stenosis geometry with non-Newtonian blood behavior. An analytical model of blood flow through a time-varying, bell-shaped stenosis in a cylindrical artery is developed in this paper to fill this research gap. It incorporates a power-law fluid model to account for the non-Newtonian properties of blood.

Key cardiovascular factors, such as velocity distribution, volumetric flow rate, pressure drop and its ratio, and wall shear stress and its ratio, are analyzed in this work under biologically relevant circumstances. Medical diagnoses and surgical procedures and the design of implants depend on an awareness of these alterations [29, 30].

Several earlier investigations have reported that increasing stenosis severity leads to reduced velocity and volumetric flow rate, accompanied by elevated pressure drop and shear stress [10–12]. The present study further extends these observations by incorporating a time-dependent bell-shaped stenosis, offering deeper insight into progressive hemodynamic changes.

II. MATHEMATICAL MODEL

In this study we examine the influence of bell-shaped arterial stenosis, which increases continuously over time, by considering axisymmetric, steady, and fully developed blood flow in a vessel with bell-shaped stenosis. Blood is considered a non-Newtonian, incompressible fluid exhibiting complex flow behavior.

We use the Navier-Stokes equations to develop a mathematical model that analyzes blood flow through a stenosed artery. Blood's shear-thinning behavior at low shear rates leads to its treatment as a non-Newtonian fluid, which is best captured by the power-law model.

A. Geometry of stenosed artery

We describe here the time-dependent geometry of symmetric, Gaussian-shaped stenosis in a blood vessel.

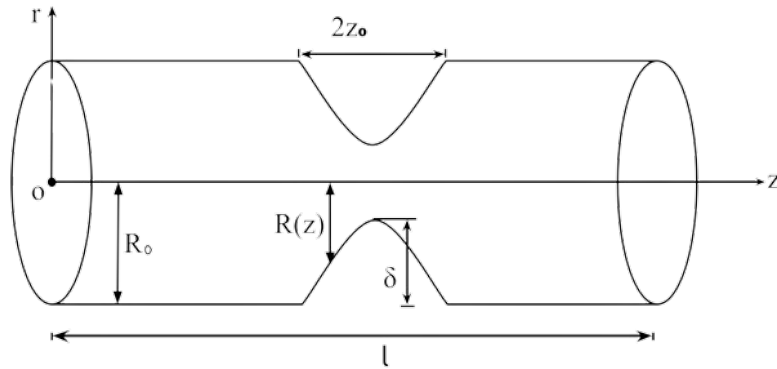


Fig. 1: Representative geometry of a stenosed artery with a bell-shaped constriction.

The radius of the vessel, varying with axial position z and time t , is given by

$$\frac{R}{R_0} = \begin{cases} 1 - \frac{\delta}{R_0} (1 - \exp(-t/T)) \exp\left(-\frac{w^2 \varepsilon^2 z^2}{R_0^2}\right), & \text{for } |z| \leq z_0, \\ 1, & \text{for } |z| \geq z_0. \end{cases} \quad (1)$$

Here, we denote $R(z, t)$ the radius of the artery with stenosis as a function of axial position ' z ' and time ' t ', R_0 the radius of the artery without stenosis. Here, t is time and δ is the maximum narrowing of stenosis. The term $(1 - e^{-t/T})$, also called the temporal term, has a transient effect representing the development of the stenosis over time and varies from 0 to 1 as t runs from 0 to ∞ . Here, t denotes time representing the yearly progression of stenosis, and T is a fixed reference time used to remove dimensions from the quantity.

When $t = 0$, the temporal term is 0, which indicates the initial state. For $t < T$, the value becomes small, and then its transient effect develops slowly. If $t = T$, its value $(1 - e^{-1}) \approx 0.632$, meaning approximately 63.2% of the vessel is affected, and the stenosis begins to show a significant effect.

When t becomes much larger than T , the term $e^{-t/T}$ tends to zero, and the effect of time becomes negligible as the system approaches complete occlusion. The impact of time is greater at the beginning and slows down gradually for very large t . Make this sentence short, simple, and academic. When t becomes much larger than T , the term $e^{-t/T}$ tends to zero, the system approaches total occlusion, and time has a negligible effect. At first, time has a greater impact, but

it decreases gradually with increasing t .

The term $\exp\left(-\frac{w^2 \varepsilon^2 z^2}{R_0^2}\right)$ represents a bell-shaped and symmetric stenosis with maximum height at $z = 0$ and gradually decreasing along the downstream direction. Here w and ε denote the stenosis width and shape parameters, respectively.

B. Velocity for non-Newtonian fluid

In this study, we analyzed blood flow through a circular artery by treating it as a non-Newtonian fluid described by the power-law model. A control volume within the artery was examined to determine the shear stress (τ) on its outer boundary which is,

$$\tau = -\mu \left(\frac{dv}{dr}\right)^n, \quad (2)$$

where μ is the dynamic viscosity, v is the axial velocity, r is the radial coordinate, and n is the flow behavior index that characterizes the non-Newtonian nature of blood. The pressure gradient along the axial direction, denoted by $P = -\frac{\partial p}{\partial z}$ is assumed to drive the flow. Based on this, the shear stress can alternatively be expressed as follows

$$\tau = \frac{Pr}{2}. \quad (3)$$

By combining (2) and (3) we have

$$\frac{dv}{dr} = \left(\frac{Pr}{2\mu}\right)^{1/n}.$$

Integrating with respect to r , and taking limits from r to R we obtain

$$v = \left(\frac{P}{2\mu}\right)^{1/n} \frac{n}{(n+1)} \left(R^{1+\frac{1}{n}} - r^{1+\frac{1}{n}}\right). \quad (4)$$

The velocity reaches its peak at the centerline of the vessel ($r = 0$) and gradually decreases toward the arterial wall as the radial distance increases. Taking blood as a non-Newtonian fluid, the flow behavior index n takes values in the range $0.68 \leq n \leq 0.80$. For this study, an average value of $n = 0.75$ is used. Now from equation (4) we have

$$v = \left(\frac{P}{2\mu}\right)^{1/n} \frac{n}{(n+1)} R_0^{\frac{n+1}{n}} \left(\left(\frac{R}{R_0}\right)^{\frac{n+1}{n}} - \left(\frac{r}{R_0}\right)^{\frac{n+1}{n}} \right). \tag{5}$$

Set

$$\chi_b^t = \frac{\delta}{R_0} (1 - \exp(-t/T)) \exp\left(-\frac{w^2 \varepsilon^2 z^2}{R_0^2}\right).$$

The exponential term $1 - e^{-t/T}$ has a Taylor expansion up to the second order

$$1 - e^{-t/T} = \frac{t}{T} - \frac{1}{2} \left(\frac{t}{T}\right)^2,$$

and we denote it by $(A - B)$ with

$$A = \frac{t}{T}, \quad B = \frac{1}{2} \left(\frac{t}{T}\right)^2.$$

Similarly, the exponential term $\exp\left(-\frac{w^2 \varepsilon^2 z^2}{R_0^2}\right)$ has a Taylor expansion up to the second order

$$\exp\left(-\frac{w^2 \varepsilon^2 z^2}{R_0^2}\right) = 1 - \frac{w^2 \varepsilon^2 z^2}{R_0^2} + \frac{1}{2} \left(\frac{w^2 \varepsilon^2 z^2}{R_0^2}\right)^2.$$

Thus,

$$\exp\left(-\frac{w^2 \varepsilon^2 z^2}{R_0^2}\right) = 1 - \alpha + \frac{\alpha^2}{2}, \quad \alpha = \frac{w^2 \varepsilon^2 z^2}{R_0^2}.$$

Hence, χ_b^t can be written as

$$\chi_b^t = \frac{\delta}{R_0} (A - B) \left(1 - \alpha + \frac{\alpha^2}{2}\right). \tag{6}$$

Thus, by using (1) and (6), equation (5) becomes

$$v = \left(\frac{P}{2\mu}\right)^{1/n} \frac{n}{(n+1)} R_0^{\frac{n+1}{n}} \left((1 - \chi_b^t)^{\frac{n+1}{n}} - \left(\frac{r}{R_0}\right)^{\frac{n+1}{n}} \right).$$

Now, we apply the binomial expansion formula, and we receive (5) as

$$v = \left(\frac{P}{2\mu}\right)^{1/n} \frac{n}{(n+1)} R_0^{\frac{n+1}{n}} \left(1 - \frac{n+1}{n} \chi_b^t + \frac{n+1}{2n^2} (\chi_b^t)^2 - \left(\frac{r}{R_0}\right)^{\frac{n+1}{n}} \right).$$

C. Volumetric flow rate

The volumetric flow rate Q can be determined using the following integral

$$Q = 2\pi \int_0^R v r dr.$$

By substituting the velocity term from Equation (4) into the above equation, the resulting expression is

$$Q = 2\pi \int_0^R \left(\frac{P}{2\mu}\right)^{1/n} \frac{n}{(n+1)} \left(R^{1+\frac{1}{n}} - r^{1+\frac{1}{n}}\right) r dr.$$

After integrating, we get

$$Q = \frac{n\pi}{3n+1} \left(\frac{P}{2\mu}\right)^{1/n} (R)^{\frac{3n+1}{n}},$$

which can be written as

$$Q = \frac{n\pi}{3n+1} \left(\frac{P}{2\mu}\right)^{1/n} (R_0)^{\frac{3n+1}{n}} \left(\frac{R}{R_0}\right)^{\frac{3n+1}{n}}. \tag{7}$$

Using the expressions for v given in equations (1) and (6), we have

$$Q = \frac{n\pi}{3n+1} \left(\frac{P}{2\mu}\right)^{1/n} (R_0)^{\frac{3n+1}{n}} (1 - \chi_b^t)^{\frac{3n+1}{n}}.$$

Using the binomial expansion, we define the axial velocity as

$$Q = \frac{n\pi}{3n+1} \left(\frac{P}{2\mu}\right)^{1/n} (R_0)^{\frac{3n+1}{n}} \left(1 - \frac{3n+1}{n} \chi_b^t + \frac{(3n+1)(2n+1)}{2n^2} (\chi_b^t)^2 \right).$$

D. Pressure drop and pressure drop ratio

From equation (7) we derive the pressure term as

$$P = \frac{2\mu Q^n}{R_0^{3n+1}} \left(\frac{3n+1}{n\pi}\right)^n \left(\frac{R}{R_0}\right)^{-(3n+1)}.$$

Set

$$C = \frac{2\mu Q^n}{R_0^{3n+1}} \left(\frac{3n+1}{n\pi}\right)^n, \quad \chi(t) = (1 - e^{-t/T}),$$

$$D_1 = (3n+1)\chi_t, \quad k = \frac{w^2 \varepsilon^2}{R_0^2},$$

$$D_2 = \frac{(3n+1)(3n+2)}{2} (\chi_t)^2.$$

Assume $\chi(t) < 1$. Now by using binomial expansion for the Taylor series of $\frac{R}{R_0}$ we receive

$$\begin{aligned} \left(\frac{R}{R_0}\right)^{-(3n+1)} &= (1 - \chi_t e^{-kz^2})^{-(3n+1)} \\ &\approx 1 + D_1 e^{-kz^2} + D_2 e^{-2kz^2}. \end{aligned}$$

Following the flow of blood through the narrowed section, the pressure drop ΔP can be calculated by

$$\begin{aligned} \Delta P &= \int_{-z_0}^{z_0} P dz \\ &= C \int_{-z_0}^{z_0} (1 - \chi(t)e^{-kz^2})^{-(3n+1)} dz \\ &\approx C \int_{-z_0}^{z_0} (1 + D_1 e^{-kz^2} + D_2 e^{-2kz^2}) dz. \end{aligned}$$

We integrate each term separately

$$\begin{aligned} \int_{-z_0}^{z_0} 1 dz &= 2z_0, \\ \int_{-z_0}^{z_0} e^{-kz^2} dz &\approx 2\left(z_0 - \frac{kz_0^3}{3} + \frac{k^2 z_0^5}{10}\right), \\ \int_{-z_0}^{z_0} e^{-2kz^2} dz &\approx 2\left(z_0 - \frac{2kz_0^3}{3} + \frac{2k^2 z_0^5}{5}\right). \end{aligned}$$

Thus, the pressure drop is

$$\begin{aligned} \Delta P \approx C \left(2z_0 + 2D_1 \left(z_0 - \frac{kz_0^3}{3} + \frac{k^2 z_0^5}{10} \right) \right. \\ \left. + 2D_2 \left(z_0 - \frac{2kz_0^3}{3} + \frac{2k^2 z_0^5}{5} \right) \right). \end{aligned} \tag{8}$$

In the case without stenosis, where both δ and t are zero, the pressure drop ΔP simplifies to

$$(\Delta P)_0 = 2z_0 C. \tag{9}$$

Based on equations (8) and (9), the expression for the pressure drop ratio is

$$\begin{aligned} \frac{\Delta P}{(\Delta P)_0} &= 1 + D_1 \left(1 - \frac{kz_0^2}{3} + \frac{k^2 z_0^4}{10} \right) \\ &+ D_2 \left(1 - \frac{2kz_0^2}{3} + \frac{2k^2 z_0^4}{5} \right). \end{aligned}$$

E. Shear stress and shear stress ratio

The shear stress along the wall of the stenotic region is regarded as minimum, as this location is relatively closer to the centerline of the vessel. It is mathematically defined as

$$\tau_{\min} = \frac{PR}{2}.$$

The wall shear stress on the basis of radial distance from the center

$$\tau_{\max} = \frac{PR_0}{2}.$$

Based on these definitions, the ratio of shear stresses between the stenosed and non-stenosed vessel walls can be expressed as

$$\frac{\tau_{\max}}{\tau_{\min}} = \frac{R_0}{R} = \left(\frac{R}{R_0} \right)^{-1} = (1 - \chi_b^t)^{-1}.$$

III. RESULTS AND DISCUSSION

We investigate the behavior of hemodynamic variables by applying the already discussed model formulations, specifically incorporating the time-dependent term. The following hemodynamic parameters are employed to generate the results: the arterial radius $R_0 = 2$ mm, the stenosis width parameter $\omega = 0.5 \text{ mm}^{-1}$, the pressure gradient $p = 100 \text{ mmHg}$, the location of maximum stenosis $z_0 = 1$, the stenosis height $\delta = 1.44 \text{ mm}$, the parameter characterizing shear thinning behavior $n = 0.75$, the constant time $T = 10$ years, and the stenosis shape parameter $\varepsilon = 1$.

A. Effect of time and viscosity on velocity

Figure 2 shows how velocity v along the axial direction z changes over time t under a constant blood viscosity of $\mu = 4.5 \text{ cP}$. At the beginning of the artery ($z = -1$) and at $t = 0.00$ years, the peak velocity in the absence of stenosis is 259.5 mm s^{-1} , while at the center of the stenosis ($z = 0$), the velocity decreases to 259.0 mm s^{-1} . This shows that the decrease in velocity is negligible when $t = 0$. As time progresses, the velocity at the arterial entry decreases to $223.1, 192.9,$ and 167.8 mm s^{-1} at $t = 1.0, 2.0,$ and 3.0 years, respectively.

At the peak of the stenosis, the corresponding velocities are $220.9, 189.0,$ and 162.6 mm s^{-1} . Over this period, the velocity decreases by approximately 35.34% at the upstream region and 37.34% at the center of the stenosis. These observations demonstrate that increasing stenosis severity leads to a progressive reduction in flow velocity, consistent with the expected hemodynamic consequences of arterial narrowing.

Figure 2B quantifies the impact of blood viscosity on flow velocity in a stenosed artery along the axial direction ' z ' at a fixed time $t = 3$ years and at $r = 0$ or at the center of the artery. According to Nader et al. [3], blood viscosity lies in between $\mu = 3.50 \text{ cP}$ and 5.50 cP , so the viscosity is varied within this range. The velocity profile, evaluated at $z = \pm 1 \text{ mm}$ from the centerline, exhibits maximum values of 227.4 mm s^{-1} ($\mu = 3.50 \text{ cP}$), 190.3 mm s^{-1} ($\mu = 4.00 \text{ cP}$), 162.6 mm s^{-1} ($\mu = 4.50 \text{ cP}$), and 141.3 mm s^{-1} ($\mu = 5.00 \text{ cP}$). These results demonstrate a 37.86% velocity reduction across the tested viscosity range, highlighting the persistent influence of viscosity even at $\delta/R_0 = 0.70$.

Figure 2C displays a 3D surface plot of velocity $v(z, t)$ as a function of axial position z and time t , at $r = 0$ and fixed viscosity $\mu = 4.5 \text{ cP}$. The velocity at the peak of the stenosis ($z = 0$) gradually declines from

S.N	Time (t) [year]	velocity V at $z = -1$	velocity V at $z = 0$	difference of velocity	percentage decrease in velocity
1	0.00	259.5	259.0	0.5	0.1920
2	1.00	223.1	220.9	2.2	0.9861
3	2.00	192.9	189.0	3.9	2.0217
4	3.00	167.8	162.6	5.2	3.0989

Table 1: Analysis of velocity profile along axial direction for different times.

S.N	viscosity (μ) [cP]	velocity V at $z = -1$	velocity V at $z = 0$	difference of velocity	percentage decrease in velocity
1	3.50	234.5	227.4	7.1	3.027
2	4.00	196.3	190.3	6.0	3.056
3	4.50	167.8	162.6	5.2	3.098
4	5.00	145.8	141.3	4.5	3.086

Table 2: Analysis of velocity profile along axial direction for different viscosities.

$t = 0$ to $t = 3$ years, illustrating the time-dependent deterioration of blood flow due to stenosis progression.

Figure 2D illustrates a 3D plot of velocity $v(z, \mu)$ versus axial position z and viscosity μ , at fixed $t = 3$ years and $r = 0$. The result shows a marked decrease in velocity with increasing viscosity, particularly at the maximum thickness of the stenosis, reflecting higher resistance for more viscous blood.

In Table 1 we show the effect of increasing stenosis on velocity at different times. Velocity is measured at the beginning and at the peak of the stenosis. In fact, effect of stenosis is zero at the beginning, and it is maximum at the peak. When $t = 0$ years, velocity at the beginning is 259.5 mm s^{-1} . In this case the velocity decreases by 0.192 %. This percentage decrement in 3 years time is 3.0989%. Again, keeping the point fixed when the time increases, the percentage decrement is 35.337% at the beginning and 37.341% at the peak of the stenosis. This difference shows that the effect of time upon velocity at the peak of the stenosis is bigger by 2.004% than at the beginning.

As time progresses and stenosis severity increases, blood flow velocity decreases due to rising flow resistance, which is governed by principles of fluid mechanics. This reduction is more pronounced at the peak of the stenosis, where the cross-sectional area is minimal, resulting in greater shear stress and energy loss, as evidenced by a higher percentage drop in velocity compared to the stenosis onset.

Table 2 highlights the impact of increasing stenosis on blood flow velocity at various viscosities. Velocity measurements are taken both at the onset of the stenosis and at its peak. As expected, the influence of stenosis is

negligible at the entry point and reaches its maximum at the narrowest section. When the viscosity is $\mu = 3.5 \text{ cP}$, the velocity at the beginning measures 234.5 mm/s , with a 3.027% decline observed at the stenosis peak. This decline slightly increases to 3.086% when viscosity rises to $\mu = 5.00 \text{ cP}$.

Additionally, a comparison of velocity reductions between the two viscosity levels shows a 37.825% decrease at the onset and a 37.862% decrease at the peak. An increase in blood viscosity leads to greater internal resistance, causing a reduction in flow velocity, which becomes more noticeable at regions of maximum constriction due to enhanced shear effects. The slightly higher velocity drop at the stenosis peak reflects the greater energy loss and flow resistance in narrower regions, consistent with principles of viscous flow in fluid mechanics.

B. Effect of time and viscosity on volumetric flow rate

Figure 3A demonstrates the effect of temporal variation on volumetric flow rate (Q) in a stenotic artery along with respect to axial position ' z ' at a constant viscosity $\mu = 4.5 \text{ cP}$. At $t = 0.00$ years (baseline), volumetric flow rate (Q) is $360.4 \text{ mm}^3/\text{s}$. As stenosis develops, volumetric flow rate (Q) is $268.8 \text{ mm}^3/\text{s}$ at $t = 1.00$ years, $201.3 \text{ mm}^3/\text{s}$ at $t = 2.00$ years and $152.2 \text{ mm}^3/\text{s}$ at $t = 3.00$ years. Q decreases from $360.4 \text{ mm}^3/\text{s}$ to $152.2 \text{ mm}^3/\text{s}$ in $t = 3$ years' time, showing a consistent 25% reduction per year. The ratio $\delta/R_0 = 0.7$ remains constant, but the effective stenosis severity increases gradually from zero to its maximum as time progresses, due to the time-dependent growth function $(1 - e^{-t/T})$ in the model.

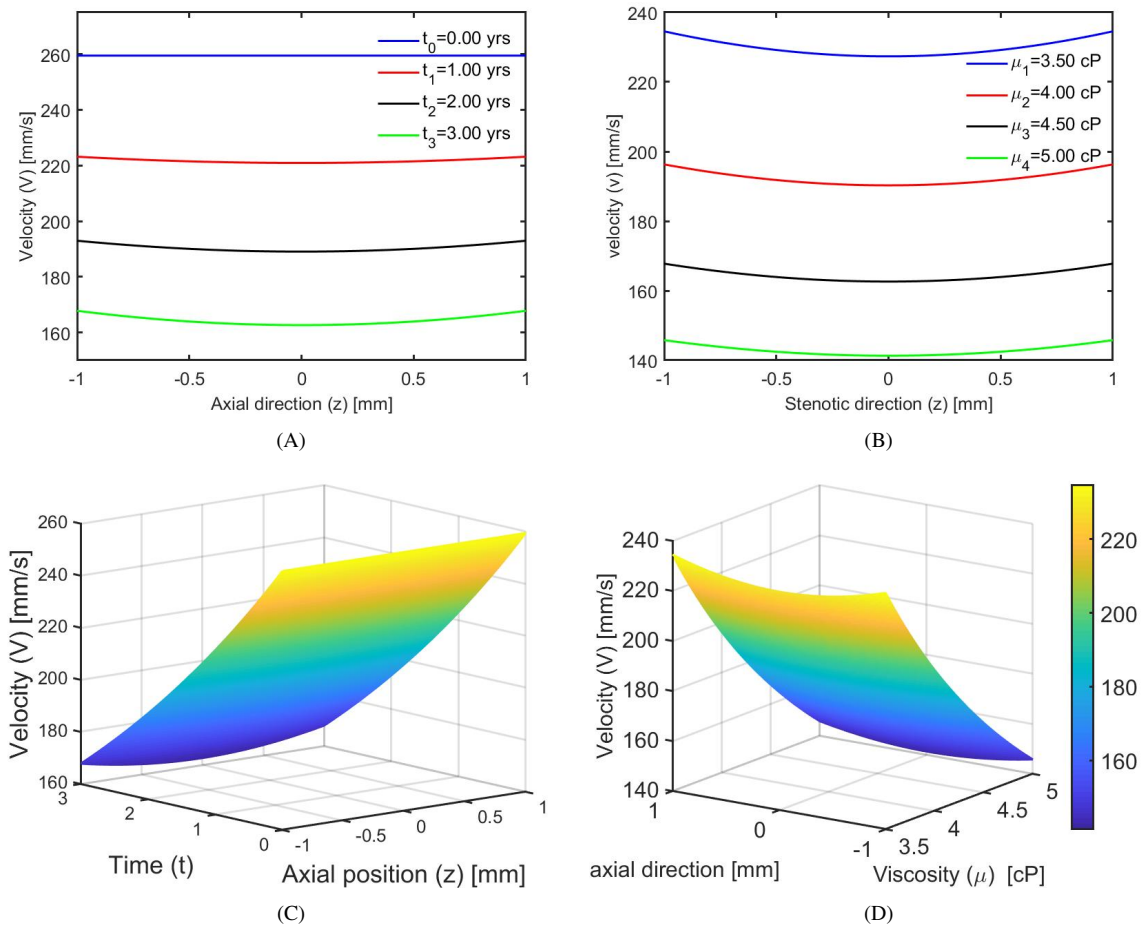


Fig. 2: Relation between velocity profile and stenosis with a time-dependent bell-shaped geometry, (A) for different times, (B) for different viscosities. Velocity due to combined effect of (C) time and stenotic height, and (D) axial direction and viscosity μ .

These results quantify the hemodynamic impact of progressive stenosis, where each 10% increase in stenosis severity corresponds to approximately 25% flow reduction. Progressive stenosis causes a significant reduction in blood flow rate over time by increasing vascular resistance, consistent with fundamental fluid dynamics principles. This study quantifies that even moderate increases in stenosis severity lead to substantial decreases in flow, highlighting the critical impact of arterial narrowing on hemodynamics.

Figure 3B demonstrates how increasing blood viscosity (μ) influences the volumetric flow rate (Q) along axial position (z) for fixed time $t = 3$ years. Using parameters same as in Fig. 3A, the flow rate is observed to decline as the viscosity increases. Specifically, when μ rises from 3.50 cP to 4.00 cP, Q decreases from 212.8

mm^3/s to 178.1 mm^3/s . Further increases in viscosity to 4.50 cP and 5.00 cP result in flow rates of 152.2 mm^3/s and 132.2 mm^3/s , respectively.

These measurements correspond to a stenosis severity ratio of $\delta/R_0 = 0.7$. The trend clearly shows that higher blood viscosity leads to a significant and consistent reduction in volumetric flow rate, emphasizing its critical role in hemodynamic behavior under stenosed conditions.

Figure 3B shows that as blood viscosity increases, the internal friction within the fluid rises, leading to greater flow resistance and a consequent decrease in volumetric flow rate. This behavior aligns with fluid mechanics principles, where higher viscosity fluids exhibit reduced flow under the same pressure gradient, especially in constricted regions like stenosed arteries.

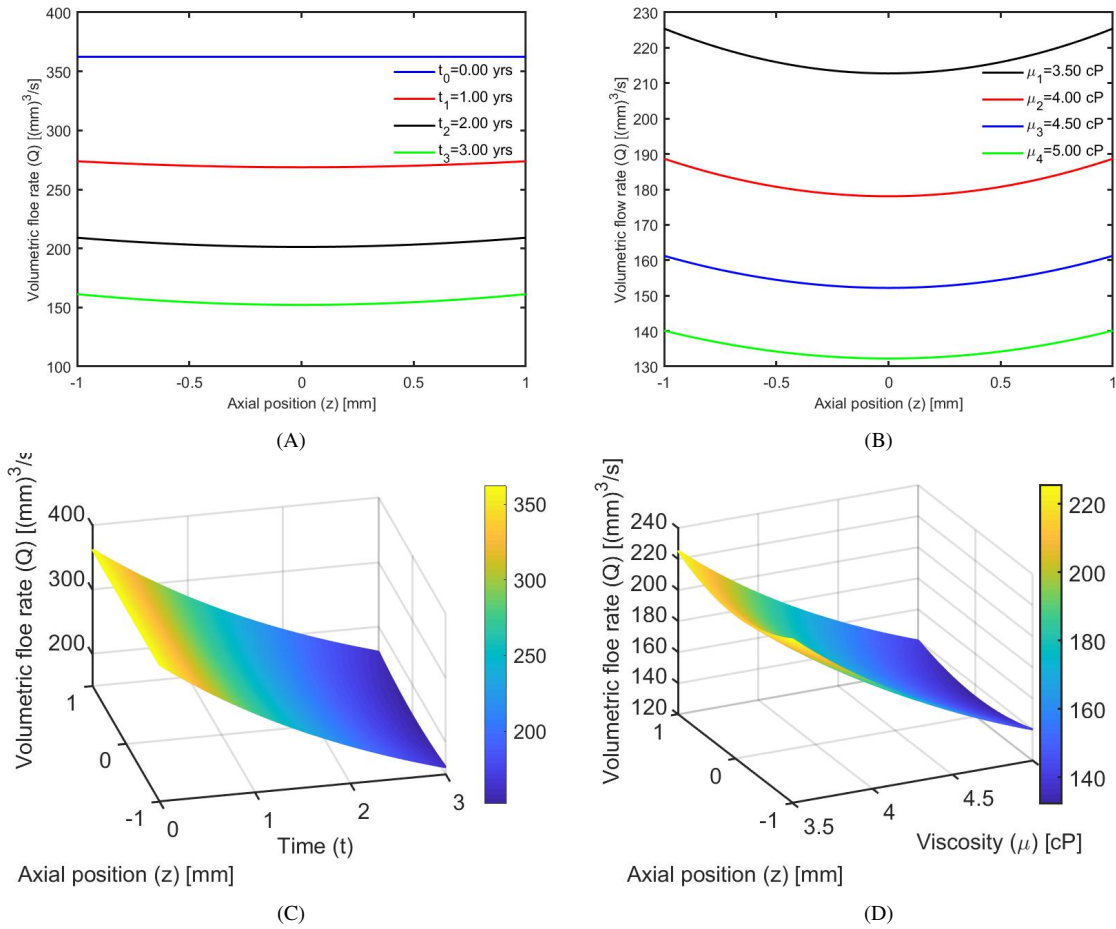


Fig. 3: Relation between volumetric flow rate and stenosis in a time-dependent bell-shaped geometry: (A) for different times, (B) for different viscosities. Volumetric flow rates under the combined effect of (C) time and axial direction and, (D) axial direction and viscosity μ .

Figures 3C and 3D display the three-dimensional surface plots of volumetric flow rate $Q(\mu, z)$ and $Q(t, z)$, respectively. In the $Q(t, z)$ plot, viscosity is fixed at $\mu = 4.5$ cP, while time varies from $t = 0.00$ to 3.00 years. The flow rate is initially high when the artery is healthy, reaching a maximum of about $362.4 \text{ mm}^3/\text{s}$ at $z = \pm 1 \text{ mm}$ and $t = 0$, but steadily decreases near $z = 0$ as the stenosis progresses, dropping to a minimum of approximately $161.2 \text{ mm}^3/\text{s}$ by $t = 3.00$ years. In contrast, the $Q(\mu, z)$ plot holds time fixed at $t = 3.00$ years while varying viscosity from $\mu = 3.50$ to 5.00 cP. The flow rate is highest (about $212.8 \text{ mm}^3/\text{s}$) at low viscosity and outer axial positions ($z = \pm 1 \text{ mm}$), but decreases sharply with increasing viscosity, reaching around $132.2 \text{ mm}^3/\text{s}$ at $\mu = 5.00$ cP and $z = 0$, where stenosis is most severe.

Both plots show symmetric bell-shaped dips centered at $z = 0$, and a smooth downward trend along increasing t or μ axes. Blood viscosity has an immediate and strong effect on reducing flow through the stenosed artery, causing sharp declines in Q as μ increases, especially at the stenosis center. In contrast, time-dependent stenosis growth leads to a gradual decline in flow over several years, reflected in the nearly linear or gently sloping nature of Q versus time.

C. Effect of time and viscosity on pressure drop (ΔP)

Figure 4A visualizes the pressure drop (ΔP) along the axial position of a stenosed artery over time using a non-Newtonian (power-law) blood flow model. The dynamic viscosity of blood is $\mu = 4.5$ cP, under a constant volumetric flow rate of $Q = 151 \text{ mm}^3/\text{s}$. At

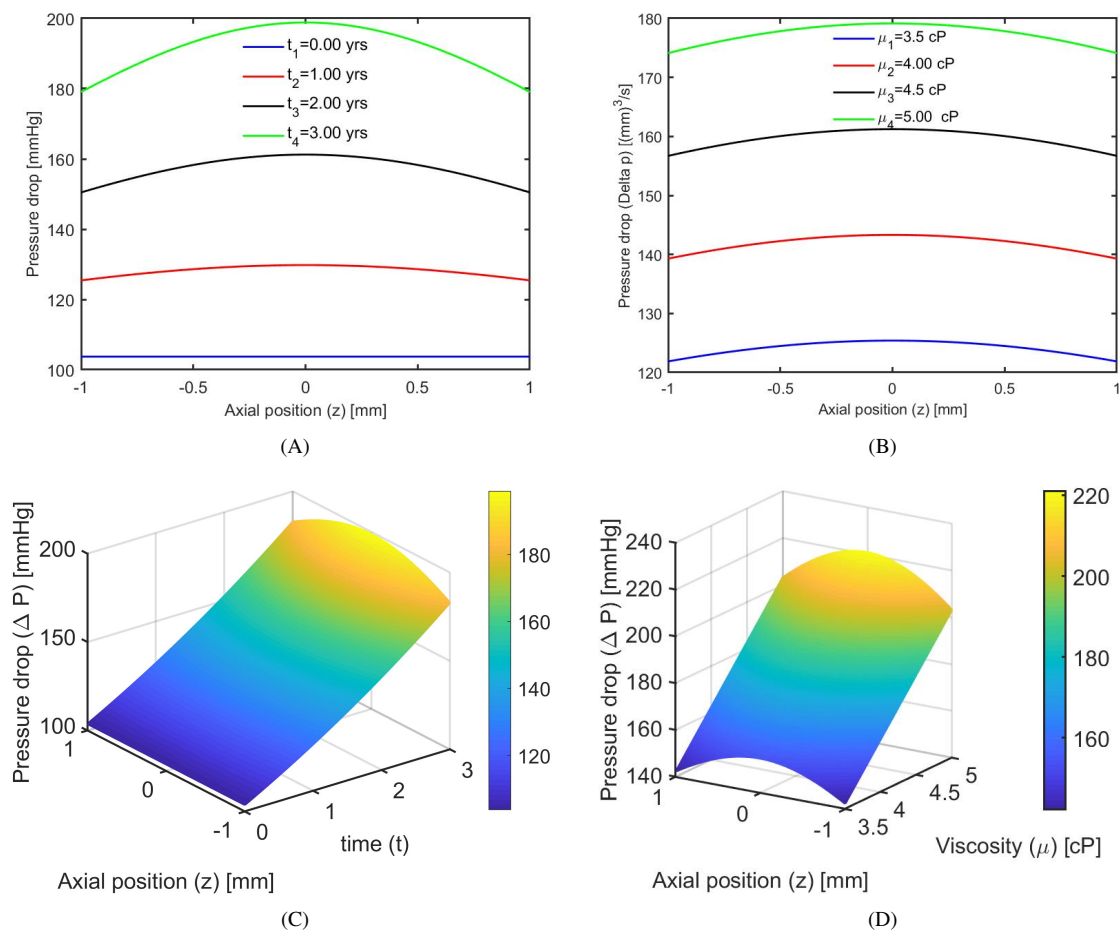


Fig. 4: Relation between pressure drop and stenosis with a time-dependent bell-shaped geometry, (A) for different times, (B) for different viscosities. Pressure drop due to combined effect of (C) time and axial direction and, (D) axial direction and viscosity μ .

baseline ($t = 0.00$ years), the pressure drop is 103.7 mmHg. As the stenosis progresses, it increases to 129.8 mmHg at $t = 1.00$ years, 161.2 mmHg at $t = 2.00$ years, and 198.8 mmHg at $t = 3.00$ years, showing an approximate 20% increase per year.

As stenosis progresses, the narrowing of the artery increases flow resistance, causing a significant rise in pressure drop along the vessel, consistent with fluid dynamics principles for viscous, non-Newtonian flow. The increasing pressure drop over time reflects the greater energy loss needed to maintain a constant flow rate through the increasingly constricted artery.

Figure 4B illustrates how increasing blood viscosity (μ) affects the pressure drop (ΔP) along the axial position (z) of a stenosed artery at a fixed time of $t = 2.00$ years. The arterial geometry and flow parameters are

the same as those used in the analysis of Figure 4A. An increase in blood viscosity from 3.50 cP to 4.00 cP results in the pressure drop rising from 125.4 mmHg to 143.2 mmHg. Subsequent increases in viscosity to 4.50 cP and 5.00 cP lead to further elevation of the pressure drop to 161.2 mmHg and 179.1 mmHg, respectively.

This behavior illustrates that elevated viscosity substantially enhances flow resistance, stressing the key role of blood's physical properties on pressure drops in narrowed blood vessels. Increasing blood viscosity raises the internal friction of blood flow, which significantly increases the pressure drop needed to maintain flow through a stenosed artery. This highlights how the physical property of viscosity directly influences flow resistance and energy loss in constricted vessels, consistent with fluid mechanics principles.

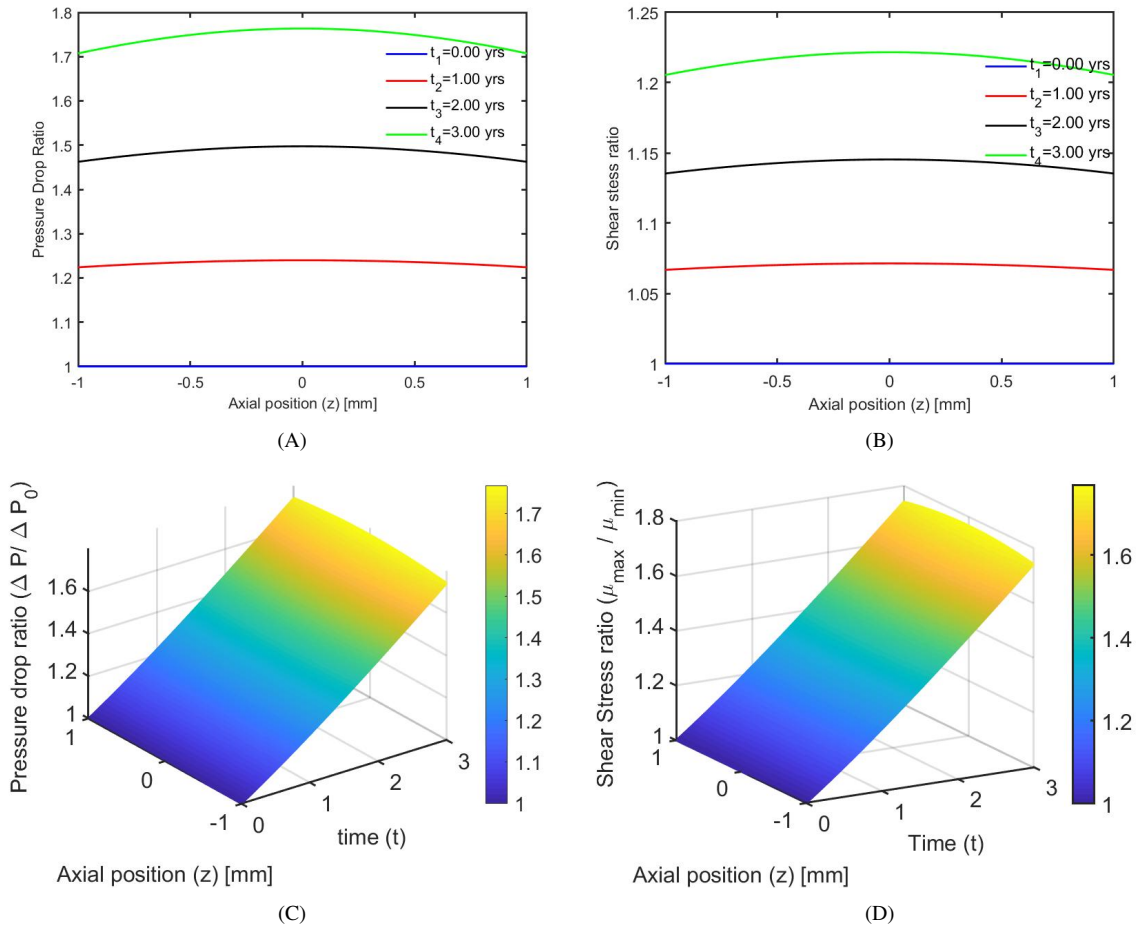


Fig. 5: Relation between (A) pressure drop ratio / (B) shear stress ratio and axial position of the stenosis with a time-dependent bell-shaped geometry for different times. Combined effect of time and axial position for (C) pressure drop ratio and (D) shear stress ratio $\frac{\tau_{max}}{\tau_{min}}$.

Figures 4C and 4D illustrate the variation of pressure drop ΔP along the artery's axial position z influenced by time and viscosity, respectively. In the time-dependent plot $\Delta P(t, z)$ at a fixed viscosity of $\mu = 4.5$ cP, the pressure drop starts at a minimum value of approximately 104.6 mmHg and steadily rises as stenosis progresses, reaching a maximum near 198.8 mmHg at the stenosis center ($z = 0$) after 3 years.

This increase reflects the gradual intensification of flow resistance due to the growing arterial narrowing. Conversely, the viscosity-dependent plot $\Delta P(\mu, z)$, keeping time fixed at 3 years, shows that pressure drop increases sharply with blood viscosity. The minimum pressure drop near the artery's ends ($z = \pm 1$) is around 148.6 mmHg, while the maximum pressure at the stenosis core reaches 220.9 mmHg at $\mu = 5.0$ cP,

indicating the strong influence of blood flow dynamics on pressure drop in stenosed arteries. Blood viscosity and duration have a significant effect on the pressure drop across a stenosed artery.

The pressure drop increases gradually with time-dependent stenosis, but it rises more sharply and instantly with increased viscosity, particularly near the arterial constriction.

D. Effect of time on pressure drop ratio

Figure 5A presents how the pressure drop ratio $\frac{\Delta P}{\Delta P_0}$ changes along the axial position (z) for different time points, while maintaining constant parameters such as radius, viscosity, and flow rate, as used in Figure 5A. The analysis considers a fixed stenosis severity level of $\frac{\delta}{R_0} = 0.7$. As time advances, the stenosis

thickens gradually in accordance with an exponential growth model. This progression leads to a consistent and measurable increase in the pressure drop ratio along the length of the artery. At the initial time $t = 0.00$ years, the pressure drop ratio begins at a baseline value of 1. As time moves forward $t = 1.00, 2.00,$ and 3.00 years, the corresponding ratios rise to 1.24, 1.49, and 1.76 respectively. This pattern reflects the accumulating influence of stenosis increasing over time on the pressure drop ratio.

Figure 5C shows how the pressure drop ratio $\frac{\Delta P}{\Delta P_0}$ changes over time along the artery's axial location z . A bell-shaped narrowing with a center at $z = 0$ that grows gradually over time with a time constant of $T = 10$ years is used to depict the course of stenosis. At $t = 0$, the pressure drop ratio is approximately 1, which indicates a healthy artery. After three years, it rises gradually to a high value of approximately 1.811 near the stenosis center. The pressure drop ratio increases steadily with time, attaining its maximum at the peak of the stenosis and remaining lower near the left and right endpoints. The gradual start of arterial narrowing and the localized rise in flow resistance as stenosis increases are reflected in this 3D Fig.

E. Effect of time on shear stress ratio

Figures 5B and 5D present two-dimensional and three-dimensional representations of how the shear stress ratio evolves along the axial coordinate z of a stenosed artery over time. The arterial narrowing is modeled in a symmetric, bell-shaped function, intensifying gradually with time based on the exponential term $1 - \exp(-t/T)$, where $T = 10$ years characterizes the rate of stenosis development. In the 2D plot (Figure 5B), distinct curves represent shear stress ratios at different time snapshots, showing a uniform rise from 1.000 at $t = 0.00$ to 1.071, 1.145, and 1.222 at $t = 1.00, 2.00,$ and 3.00 years, respectively.

The 3D plot (Figure 5D) complements this by showing a smooth, upward-sloping surface, where shear stress increases both with time and toward the stenosis center ($z = 0$). The progressive increase in stress and geometric symmetry around the center emphasizes how stenosis exacerbates the effects on wall mechanics. All of these figures together show that shear stress increases gradually in response to stenosis that develops over time, reaching its maximum at the wall where the stenosis has its maximum height. Time-dependent and spatially localized stenosis raises the mechanical difficulties associated with progressive arterial narrowing.

IV. CONCLUSION

In this work we have examined the effect of increasing thickness of the stenosis on hemodynamics when blood passes through a bell-shaped stenosis. Blood is modeled as a non-Newtonian, incompressible, viscous fluid following a power-law rheology. Assuming axisymmetric flow, a mathematical model based on the Navier-Stokes equations is formulated to investigate velocity, pressure drop, pressure drop ratio, volumetric flow rate, and shear stress ratio.

The results reveal that both time progression and increasing blood viscosity significantly reduce velocity in a stenosed artery. As we move from the center towards the arterial wall, the velocity decreases gradually. However, the effect of time-dependent progression of stenosis is more dominant. The volumetric flow rate is significantly reduced by blood viscosity, particularly in the stenotic region.

Thus, stenosis severity over time has a greater impact on hemodynamic behavior than viscosity variation. In contrast, time-dependent stenosis growth leads to a gradual decline in flow over several years, reflected in the nearly linear or gently sloping nature of Q versus time. Pressure drop gradually rises over time but reacts more strongly to variations in viscosity. The shear stress shows that there is a growing and focused mechanical pressure caused by the worsening of stenosis, which increases over time and is highest at the peak of the stenosis. These results highlight how rheological and temporal factors interact and compound to affect circulatory flow dynamics.

The present results align well with our previous studies on non-Newtonian blood flow in stenosed arteries, showing reduced velocity and volumetric flow rate and increased pressure drop and shear stress with greater stenosis severity. By incorporating time-dependent bell-shaped stenosis, this study reveals a more progressive deterioration of hemodynamic characteristics over time. These trends are also consistent with other studies discussed in the introduction. Including temporal progression provides further insight into the long-term hemodynamic impact of stenosis, complementing and extending existing models. This result may be useful in the clinical approach as well as for researchers in this field.

ACKNOWLEDGMENT

Jeevan Kafle acknowledges the financial support through Major Research Grant from the Research Directorate, Rector Office, Tribhuvan University, Kathmandu, Nepal.

REFERENCES

- [1] N. Antonova, A. Alexandrova, G. Melnikova, A. Petrovskaya, et al., Micromechanical properties of peripheral blood cells (erythrocytes, lymphocytes and neutrophils) in patients with diabetes mellitus type 2, examined with atomic force microscope (AFM), *Series on Biomechanics*, 33(4):3–11, 2019.
- [2] H. L. Goldsmith, J. Marlow, F. C. MacIntosh, Flow behaviour of erythrocytes – I. Rotation and deformation in dilute suspensions, *Proceedings of the Royal Society of London. B. Biological Sciences*, 182:351–384, 1972.
- [3] E. Nader, S. Skinner, M. Romana, R. Fort, N. Lemonne, N. Guillot, et al., Blood Rheology: Key Parameters, Impact on Blood Flow, Role in Sickle Cell Disease and Effects of Exercise, *Frontiers in Physiology*, 10:01329, 2019.
- [4] T. J. Pedley, *The Fluid Mechanics of Large Blood Vessels*, Cambridge University Press, 2008.
- [5] D. E. Mohrman, L. J. Heller, *Cardiovascular Physiology, Ninth Edition*, McGraw-Hill Education, 2018.
- [6] V. Kashyap, B. B. Arora, S. Bhattacharjee, A computational study of branch-wise curvature in idealized coronary artery bifurcations, *Applications in Engineering Science*, 4:100027, 2020.
- [7] S. Chakravarty, Effects of stenosis on the flow-behaviour of blood in an artery, *International Journal of Engineering Science*, 25:1003–1016, 1987.
- [8] D. F. Young, N. R. Cholvin, R. L. Kirkeeide, A. C. Roth, Hemodynamics of arterial stenoses at elevated flow rates, *Circulation Research*, 41:99–107, 1977.
- [9] P. N. Gautam, J. Kafle, Effect of curvature on hemodynamics in a stenotic artery, *BIOMATH*, 14:2501175, 2025.
- [10] N. Antonova, X. Dong, P. Tosheva, E. Kaliviotis, I. Velcheva, Numerical analysis of 3D blood flow and common carotid artery hemodynamics in the carotid artery bifurcation with stenosis, *Clinical Hemorheology and Microcirculation*, 57:159–173, 2014.
- [11] A. Buradi, A. Mahalingam, Effect of Stenosis Severity on Wall Shear Stress Based Hemodynamic Descriptors using Multiphase Mixture Theory, *Journal of Applied Fluid Mechanics*, 11:1497–1509, 2018.
- [12] B. Liu, The influences of stenosis on the downstream flow pattern in curved arteries, *Medical Engineering & Physics*, 29:868, 2007.
- [13] D. F. Young, Effect of a Time-Dependent Stenosis on Flow Through a Tube, *Journal of Manufacturing Science and Engineering*, 90:248–254, 1968.
- [14] D. N. Ku, D. P. Giddens, C. K. Zarins, S. Glagov, Pulsatile flow and atherosclerosis in the human carotid bifurcation. Positive correlation between plaque location and low oscillating shear stress, *Arteriosclerosis, Thrombosis, and Vascular Biology*, 5:293–302, 1985.
- [15] J.-S. Lee, Y.-C. Fung, Flow in Locally Constricted Tubes at Low Reynolds Numbers, *Journal of Applied Mechanics*, 37:9–16, 1970.
- [16] J. Kafle, H. P. Gaire, P. R. Pokhrel, P. Kattel, Analysis of blood flow through curved artery with mild stenosis, *Mathematical Modeling and Computing*, 9:217–225, 2022.
- [17] A. Muravyov, P. Mikhailov, I. Tikhomirova, S. Bulaeva, V. Zinchuk, R. Ostroumov, Microrheological responses of red blood cells to gaseous mediators under physiological and pathophysiological conditions, *Series on Biomechanics*, 36:21–31, 2022.
- [18] N. Antonova, D. Xu, I. Velcheva, E. Kaliviotis, P. Tosheva, Stenosis effects on the fluid mechanics of the common carotid artery bifurcation for unsteady flows, *Journal of Mechanics in Medicine and Biology*, 15:1540008, 2015.
- [19] S. Schilt, J. E. Moore Jr, A. Delfino, J.-J. Meister, The effects of time-varying curvature on velocity profiles in a model of the coronary arteries, *Journal of Biomechanics*, 29:469–474, 1996.
- [20] P. N. Gautam, C. Pokharel, T. B. Rana, J. Kafle, Hemodynamics in a curved artery with mild stenosis: A two-layered model, *International Journal of Thermofluids*, 27:101253, 2025.
- [21] A. Bhatnagar, S. Agarwal, R. K. Shrivastav, J. Pal, Effect of Time Dependent Stenosis on Blood Flow through an Arterial Segment, *Turkish Journal of Computer and Mathematics Education (TURCOMAT)*, 11:1685–1691, 2021.
- [22] G. Bugliarello, J. Sevilla, Velocity distribution and other characteristics of steady and pulsatile blood flow in fine glass tubes, *Biorheology*, 7:85–107, 1970.
- [23] R. K. Dash, G. Jayaraman, K. N. Mehta, Flow in a catheterized curved artery with stenosis, *Journal of Biomechanics*, 32:49–61, 1999.
- [24] K. Haldar, H. I. Andersson, Two-layered model of blood flow through stenosed arteries, *Acta Mechanica*, 117:221–228, 1996.
- [25] D. S. Sankar, U. Lee, Two-fluid Casson model for pulsatile blood flow through stenosed arteries: A theoretical model, *Communications in Nonlinear Science and Numerical Simulation*, 15:2086–2097, 2010.
- [26] R. K. Srivastav, A. K. Agnihotri, Blood flow through a bell-shaped stenosis in catheterized arteries, *e-Journal of Science & Technology (e-JST)*, 10(1):1–11, 2015.
- [27] P. N. Gautam, C. Pokharel, G. R. Phaijoo, P. Kattel, J. Kafle, Effect of increasing stenosis over time on hemodynamics, *BIOMATH*, 12:2310067, 2023.
- [28] R. Ponalagusamy, R. Manchi, A study on two-layered (K. L.-Newtonian) model of blood flow in an artery with six types of mild stenoses, *Applied Mathematics and Computation*, 367:124767, 2020.
- [29] K. Bravo-Jaimes, N. L. Palaskas, J. Banchs, N. I. Abelhad, A. Altaf, S. Gouni, J. Song, S. A. Hassan, C. Iliescu, A. Deswal, S. W. Yusuf, Rate of Progression of Aortic Stenosis in Patients With Cancer, *Frontiers in Cardiovascular Medicine*, 8:644264, 2021.
- [30] A. C. Stamou, J. Radulovic, J. M. Buick, Effect of stenosis growth on blood flow at the bifurcation of the carotid artery, *Journal of Computational Science*, 54:101435, 2021.